Proceedings of the 17th World Congress
The International Federation of Automatic Control
Seoul, Korea, July 6-11, 2008

Novel Control Scheme for Helicopter Flight: Fuzzy Immune Adaptive Model Inversion Control

Zhao Jia, Chen Shenggong, Shen Gongzhang

School of Automation Science and Electrical Engineering, Beijing University of Aeronautics and Astronautics, Beijing, China, (e-mail: zhaojia0824@163.com, shanechen62@163.com, shengz@buaa.edu.cn)

Abstract: A novel control scheme, fuzzy immune adaptive model inversion control, was put forward, aiming at the large flight envelope curve control problem of helicopter. The proposed scheme was designed based on model inversion theory, biology immune response mechanism and fuzzy control method. It could achieve effective control throughout large flight envelope curve via the design of fuzzy immune online-compensation element, only needing a static inverse model on the basis of a single flight condition. Simulation results comparing with the neural network adaptive control method show the system based on the proposed scheme has better real-time performance. It can offer adaptive compensation in time for model inverse errors caused by the changes of flight conditions and achieve accurate commands tracking. Stronger robustness has been demonstrated in the case of control surface damage and sensor output noise. Good three-axis uncoupled performance has also been shown.

1. INTRODUCTION

Helicopter, as a kind of dynamic system characterized with strong coupling and inherently static unsteady, contains three typical flight phases (hover, low speed forward flight and high speed forward flight). There are distinct differences among the aerodynamic characteristics of the three ones, which bring challenges to the large flight envelope curve control (LFEC) problem of helicopter.

At the end of 20th century, an advanced adaptive control approach, neural network adaptive model inversion control (NNAMIC), had been developed to solve the LFEC problem of helicopter (Nakwan K. and Anthony J.C., 2004; Nilesh A. S. and Joseph F.H., 2004). The neural network is utilized to adaptive cancelling the effect from inversion errors in flight, and effective control could be achieved through large flight envelope curve. Nevertheless, some limitations still exist: poor real-time performance, low anti-interference feature, difficulties in selecting training samples, etc.

Artificial immune system (AIS) is a new theory based on biology immune system (BIS), which has received wide attention in recent years (Takahashi K. and Yamada T., 1998; Jun Li, Hui Yan and Guoqing Tang, 2004; Liu Liqun and Sun Zhiyi, 2007). AIS belongs to a kind of adaptive system with strong robustness, and it can maintain stability in some complex dynamic environments in which there may be kinds of uncertain factors and disturbances. The mechanism of AIS shed some new light on treating with complicated dynamic problems.

To overcome the shortcomings of NNAMIC, a new control scheme, fuzzy immune adaptive model inversion control (FIAMIC), was proposed in this paper. Furthermore, comparison simulation experiments with NNAMIC have also been done aiming at the helicopter LFEC problem. Simulation results show the feasibility and advantages of the proposed scheme.

2. FUZZY IMMUNE ADAPTIVE MODEL INVERSION CONTROL SCHEME

FIAMIC scheme is established on the basis of traditional model inversion control theory (Nakwan K. and Anthony J.C., 2004; Nilesh A.S. and Joseph F.H., 2004). Attitude command attitude hold (ACAH) response type is implemented for flight control system. As the design schemes of three-axis attitude angle channels control are similar, only the design structure of pitch angle channel is given as an example (Fig. 1).

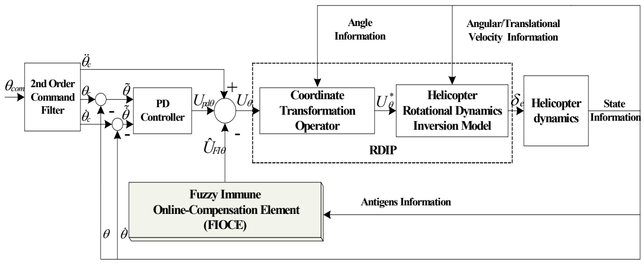

Fig. 1. Structure of FIAMIC system for pitch angle channel

As shown in Fig.1, RDIP stands for rotational dynamics inversion processor and plays the role of approximate inversion model of the helicopter. The complete pseudo control signal for the pitch angle attitude ACAH control system is

$$U_\theta = U_{pd\theta} + \ddot{\theta}_c - \hat{U}_{FI\theta} \tag{1}$$

where the reference model signal $\ddot{\theta}_c$ is the pitch angle acceleration expected. $\hat{U}_{FI\theta}$ is the adaptive signal provided by fuzzy immune online-compensation element (FIOCE). The

978-1-1234-7890-2/08/$20.00 © 2008 IFAC 10.3182/20080706-5-KR-1001.1853

PD controller output $U_{pd\theta}$ is acting on the tracking error. We can describe $U_{pd\theta}$ as

$$U_{pd\theta} = K_d \dot{\tilde{\theta}} + K_p \tilde{\theta} \tag{2}$$

where K_p, K_d are positive real number and $\tilde{\theta} \triangleq \theta_c - \theta$.

Defining $\Delta \triangleq \ddot{\theta} - U_\theta$, where Δ stands for the inversion error between RDIP and the helicopter. Equation (3) could be obtained by putting Δ into (1).

$$\ddot{\tilde{\theta}} + K_d \dot{\tilde{\theta}} + K_p \tilde{\theta} = \hat{U}_{FI\theta} - \Delta \tag{3}$$

The model tracking error can be expressed as $e_\theta = \begin{bmatrix} \tilde{\theta} & \dot{\tilde{\theta}} \end{bmatrix}^T$. We can describe (3) as

$$\dot{e}_\theta = A \cdot e_\theta + B\left[\hat{U}_{FI\theta} - \Delta\right] \tag{4}$$

where $A = \begin{bmatrix} 0 & 1 \\ -K_p & -K_d \end{bmatrix}$, $B = \begin{bmatrix} 0 & 1 \end{bmatrix}^T$.

As shown in (2)~(4), the system response characters in $\Delta = 0$ is decided directly by $U_{pd\theta}$, which means e_θ (here $\dot{e}_\theta = A \cdot e_\theta$) can tend to zero with an expected law in case that the inversion error Δ could be counteracted completely by adaptive signal $\hat{U}_{FI\theta}$. The design of $U_{FI\theta}$ is the core of FIAMIC. K_p and K_d should also be chosen correctly such that A can be Hurwitz matrix.

3. RDIP PRINCIPLE

For attitude dynamics of helicopter, the approximate model is generated by linearizing the nonlinear model around a flight condition and neglecting the coupling between the attitude and translational dynamics (Nakwan K. and Anthony J.C., 2004).

$$\dot{\omega}_o = A_1 \cdot x_1 + A_2 \cdot \omega + B \cdot \left(\delta_{cur} - \delta_{trim}\right) \tag{5}$$

where A_1 and A_2 are the attitude and translational dynamics respectively. B is the invertible control matrix. ω is the body angular velocity vector relative to the ground coordinates. x_1 is the body velocity vector relative to the ground coordinates. δ_{trim} is the trim control vector that is consistent with the linear model. The current control values can be evaluated as

$$\delta_{cur} = \hat{B}^{-1} \cdot (\dot{\omega}_o - \hat{A}_1 \cdot x_1 - \hat{A}_2 \cdot \omega) + \delta_{trim} \tag{6}$$

$\dot{\omega}_o$ is the body angle acceleration vector expected. For ACAH, it is determined by transforming U from the Euler coordinates to the body coordinates. $\hat{A}_1$, $\hat{A}_2$ and $\hat{B}$ are approximate values of A_1, A_2 and B respectively.

Considering the three-axis attitude angle channel, the pseudo control variables can be expressed as follow

$$U = \begin{bmatrix} U_\phi \\ U_\theta \\ U_\psi \end{bmatrix} = \begin{bmatrix} K_{p\phi}\tilde{\phi} + K_{i\phi}\dot{\tilde{\phi}} + \ddot{\phi}_c - \hat{u}_{FI\phi} \\ K_{p\theta}\tilde{\theta} + K_{i\theta}\dot{\tilde{\theta}} + \ddot{\theta}_c - \hat{u}_{FI\theta} \\ K_{p\psi}\tilde{\psi} + K_{i\psi}\dot{\tilde{\psi}} + \ddot{\psi}_c - \hat{u}_{FI\psi} \end{bmatrix} \tag{7}$$

Transforming U from the Euler frame to the body frame

$$U^* = T \cdot U \tag{8}$$

where T is the transformation operator.

Letting $U^* = \dot{\omega}_o$ and putting it into (6), we can obtain the RDIP equation

$$\Delta\delta = \delta_{cur} - \delta_{trim} = \hat{B}^{-1} \cdot (U^* - \hat{A}_1 \cdot x_1 - \hat{A}_2 \cdot \omega) \tag{9}$$

4. FIOCE DESIGN

As the core of whole system, FIOCE will simulate biology immune response mechanism and counteract the inversion error brought by RDIP in time.

4.1 Biology Immune Response Mechanism

The immune system enables human survival of infection and disease by virtue of the immune response mechanism. Immune response can be divided into two types: body fluids response and cells response, and FI online-compensation element is designed based on the former.

The body fluids immune response process can be described as shown in Fig. 2 (Takahashi K. and Yamada T., 1998), where "+" stands for activating effect and "−" stands for suppressing effect. B cells and T cells play key roles in the process of immune response. When antigens (Ag) are taken in by B cells and appear on the surface of B cells, Ag exhibit antigen presentation cells (APCS). APCS stimulate both help T cells (T_H) and suppressor T cells (Ts). T_H help B cells synthesizing and secreting antibodies (Ab) for neutralizing Ag and also promote the growth of Ts. The main function of Ts is suppressing the growth of B cells and T_H. At the initial phase of immune response, the concentration of Ag and T_H is high, and Ts is low. It results in rapid increase of B cells and Ab. With the progress of immune response, the concentration of Ag is getting low, which can lead the increase of Ts and the decrease of T_H, the amount of B cells and Ab would also decrease. Finally, the immune system will return its balance.

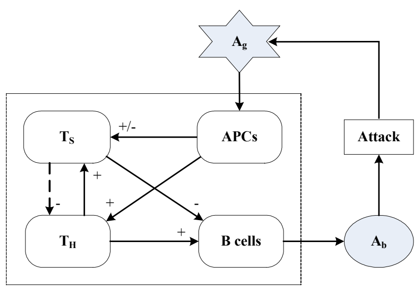

Fig. 2. Principe of body fluids immune response

Based on the above principle, the following immune feedback law is considered (Jun Li, Hui Yan and Guoqing Tang, 2004; Liu Liqun and Sun Zhiyi, 2007):

At the k[th] generation, defining the concentration of B cells as $B(k)$, the concentration of Ag and Ab as $\varepsilon(k)$ and $\zeta(k)$ respectively, the effect of T_H and Ts on B cells as $T_H(k)$ and $T_S(k)$ respectively, and then

$$B(k) = T_H(k) - T_S(k) \tag{10}$$

$$T_H(k) = K_H \cdot \varepsilon(k) \tag{11}$$

$$T_S(k) = K_S \cdot \rho_{Ag}(\varepsilon) \cdot \psi_{Ab}(\zeta) \cdot \varepsilon(k) \tag{12}$$

Where K_H is the T_H activating coefficient, K_S is the T_S suppressing coefficient. $\rho_{Ag}(\varepsilon)$ is the immune adjusting function which stands for the effect on T_S during different stages of immune response process. $\psi_{Ab}(\zeta)$ is the antigen-effect function which stands for indirect effect of Ab and T_S.

There is an approximate proportional relationship existing between the concentration of Ab and B cells

$$\zeta(k) = K \cdot B(k) \tag{13}$$

The law of body fluids immune response mechanism could be obtained by using (10)~(13).

$$\zeta(k) = K \cdot \left(K_H \cdot \varepsilon(k) - K_S \cdot \rho_{Ag}(\varepsilon) \cdot \psi_{Ab}(\zeta)\right) \cdot \varepsilon(k) \tag{14}$$

4.2 FI online-compensation law design

Based on the adjusting law mentioned in section 4.1, FI online-compensation law could be gained. Table 1 shows the relationship between FIOCE and BIS.

Table 1. Relationship between FIOCE and BIS

FIOCE	BIS
Sample time of system	Generations
Tracking error information	concentration of Ag
Adaptive compensation signal	concentration of Ab
Dissatisfying error demand	Activating
Satisfying error demand	Suppressing

It is clear from (4) that the appearance of Δ will result in tracking error $\tilde{\theta}$ directly. Therefore, $\tilde{\theta}$ will be considered as "inbreak antigens" and the adaptive signal $U_{FI\theta}$ will be considered as "antibodies" in this paper. Furthermore, for considering the history, present and future information of tracking error synthetically, "antigens shaping module" is designed in which concentration of antigens is expressed as shown in (15), where λ_1, λ_2 and λ_3 .are the weights parameters.

$$\varepsilon(k) = \begin{bmatrix} \lambda_1 & \lambda_2 & \lambda_3 \end{bmatrix} \cdot \begin{bmatrix} \int \tilde{\theta}(k)dk & \tilde{\theta}(k) & \dot{\tilde{\theta}}(k) \end{bmatrix}^T \tag{15}$$

FI online-compensation law (16) could be obtained from (14), (15), and Table 1.

$$\left.\begin{aligned} U_{FI}(k) &= K \cdot \left(K_H - K_S \cdot \rho_{Ag}(\varepsilon) \cdot \psi_{Ab}(U_{FI})\right) \cdot \varepsilon(k) \\ \varepsilon(k) &= \lambda_1 \cdot \int \tilde{\theta}(k)dk + \lambda_2 \cdot \tilde{\theta}(k) + \lambda_3 \cdot \dot{\tilde{\theta}}(k) \end{aligned}\right\} \tag{16}$$

Fig. 3 shows the structure of FIOCE.

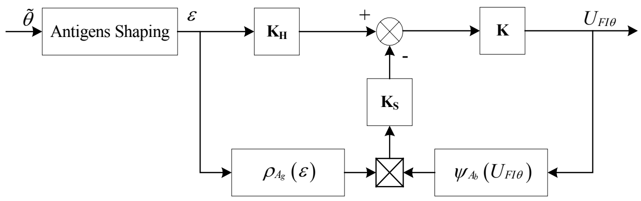

Fig. 3. Structure of FIOCE

4.3 Antigen-effect function design

The adjusting effect between T_S and antibodies is complex such that no mature method has been developed to describe it. Fuzzy controller has been proved to be a kind of universal functional approximators. So it is an effective method to construct nonlinear functional approximator.

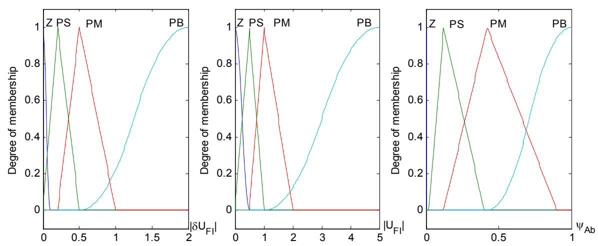

Fig. 4. Degree of memberships for input/output

Table 2. Fuzzy controller rules

$\lvert \dot{U}_{FI\theta} \rvert$ \ $\lvert U_{FI\theta} \rvert$	Z	PS	PM	PB
Z	Z	Z	PS	PS
PS	Z	PS	PS	PM
PM	PS	PS	PM	PB
PB	PS	PM	PB	PB

A fuzzy controller is designed here to implement the nonlinear function $\psi_{Ab}(U_{FI\theta})$. It consists of two inputs and one output. The input variables are the FI online-compensation signal $U_{FI\theta}(k)$ and its derivative $\dot{U}_{FI\theta}(k)$. The output variable is the value of the antigen-effect function ψ_{Ab}. According to the T_S adjusting mechanism, the membership functions of inputs and output are defined as shown in Fig. 4, and the fuzzy rules are defined as shown in Table 2. In the rules, Zadeh fuzzy logic AND operators are used. Max-Min method is used for fuzzy inference and centroid defuzzification method is used for calculating the output.

4.4 Immune adjusting function design

According to immune response mechanism, at the stage of immune activation, the concentration of antigens is high and T_S is suppressed. Nevertheless, the concentration of antigens is proper low and T_S is activated at the stage of immune suppression. When the concentration of antigens gets low enough, organism will be in the stage of immune stability.

Based on above principle, the immune adjusting function can be defined as shown in (17), where ρ_{Ag}^{-} is the immune-suppression factor and ρ_{Ag}^{+} is the immune- activation factor.

$$\rho_{Ag}(\varepsilon) = \rho_{Ag}^{-}(\varepsilon) - \rho_{Ag}^{+}(\varepsilon) \tag{17}$$

$$\rho_{A_g}^{-} = \begin{cases} 0 & , \ |\varepsilon(k)| \in [0 \quad \varepsilon_0] \cup [\varepsilon_2 \quad +\infty) \\ \dfrac{|\varepsilon| - \varepsilon_0}{\varepsilon_1 - \varepsilon_0} & , \ |\varepsilon(k)| \in [\varepsilon_0 \quad \varepsilon_1] \\ \dfrac{\varepsilon_2 - |\varepsilon|}{\varepsilon_2 - \varepsilon_1} & , \ |\varepsilon(k)| \in [\varepsilon_1 \quad \varepsilon_2] \end{cases} \tag{18}$$

$$\rho_{A_g}^{+} = \begin{cases} 0 & , \ |\varepsilon(k)| \in [0 \quad \varepsilon_1] \\ \dfrac{|\varepsilon| - \varepsilon_1}{\varepsilon_2 - \varepsilon_1} & , \ |\varepsilon(k)| \in [\varepsilon_1 \quad \varepsilon_2] \\ 1 & , \ |\varepsilon(k)| \in [\varepsilon_2 \quad +\infty) \end{cases} \tag{19}$$

5. NUMERICAL RESULTS AND ANALYSIS

The ACAH system for pitch angle channel shown in Fig.1 has been implemented on the full flight envelope curve model of PUMA-XW241 helicopter using Maltab7.1/Simulink. The structure of 2nd order command filter is shown in Fig. 5, where the parameters (ξ, ω_n) are chosen based on ADS-33E (Anon, 2000). RDIP element is designed on the basis of hover.

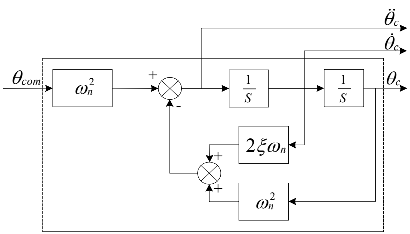

Fig. 5. Structure of 2nd order command filter

NNAMIC method (Nilesh A.S. and Joseph F.H., 2004) has also been implemented for the simulation experiments comparing with FIAMIC scheme proposed in this paper.

In following sections, the system designed based on FIAMIC is called "FI system" for short, the system designed based on NNAMIC is called "NN system", and the system without adaptive compensation element is called "original system". Once achieving design, all control parameters in the three systems keep invariable.

5.1 LFEC simulation for ACAH mode

The simulation is done for checking the adaptive compensation ability of FIOCE in case that the flight conditions have been changed. Three typical flight conditions have been chosen for simulation: hover, low speed forward flight (20knots, 40knots) and high speed forward flight (100knots, 120knots and 150knots). As length limitation, only the results of hover, 40knots, and 150knots are shown.

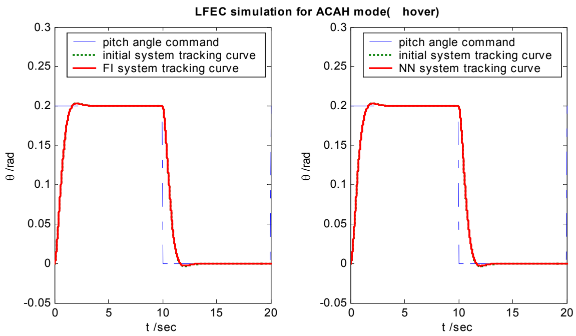

Fig. 6-a. Pitch angle tracking curves for FIOCE (hover)

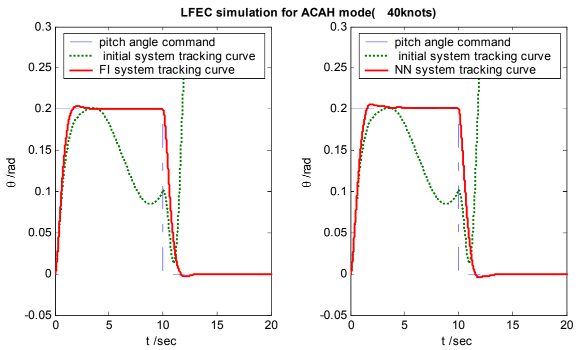

Fig. 6-b. Pitch angle tracking curves for FIOCE (40knots)

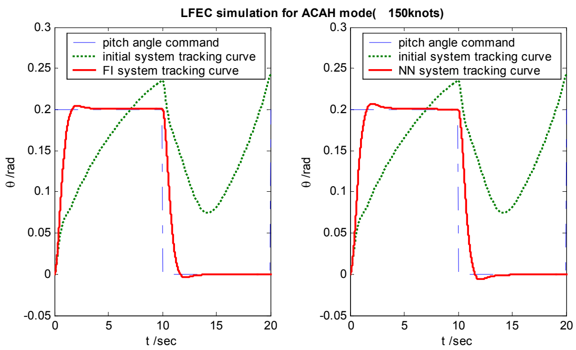

Fig. 6-c. Pitch angle tracking curves for FIOCE (150knots)

Fig. 6-a shows the pitch angle tracking curves at hover. The responses of FI system, NN system and original system are highly similar and all achieve control aiming well. It demonstrates that RDIP could describe the inversion model of

helicopter appropriately at hover, and the compensation effects of both FI online-compensation element and NN element are not obvious. Fig. 6-b and Fig. 6-c show the curves at 40konts and 150knots forward flight respectively. In these phases, RDIP could not be able to describe the inversion model appropriately and result in the appearance of inversion errors. The response curves of original system are divergent; nevertheless, both FI and NN system could compensate the inversion errors bought by the changes of flight condition in time and implement command tracking well.

5.2 Simulation for control surface damage

This simulation in this section is done for checking the fault-tolerance ability of system in case of the existing of control surface damage.

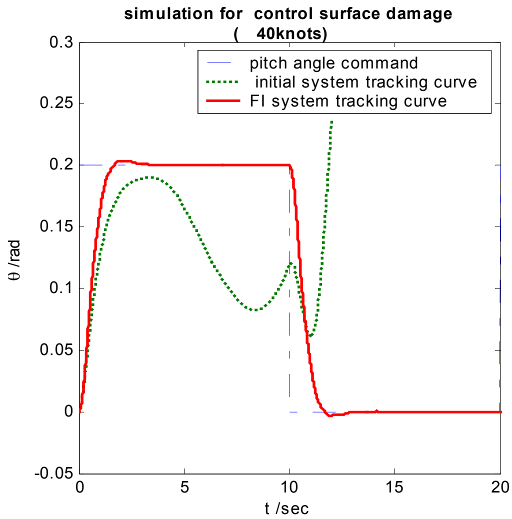

Fig. 7-a. Simulation for control surface damage in FI system

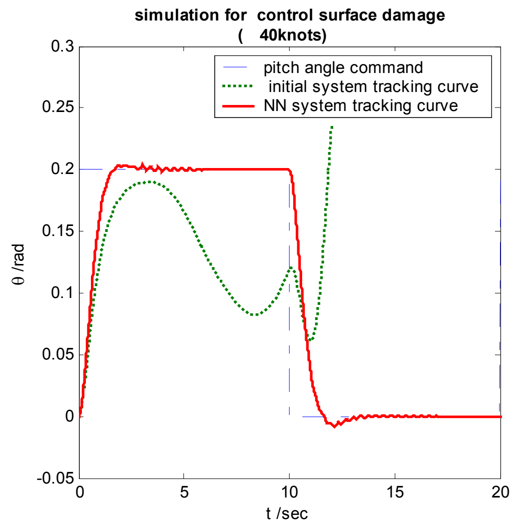

Fig. 7-b. Simulation for control surface damage in NN system

Fig. 7-a and Fig. 7-b show response curves of the three systems at 40konts forward flight when there is 20% decrease of control surface. With the effects caused by descending of control surface, the response curve of original system is divergent, and small-amplitude fluctuation is appeared in the response curve of NN system during the initial phase of command tracing process (Fig. 7-b), however, FI system could still implement command tracking quite well (Fig. 7-a).

5.3 Simulation for anti-interference capability

The simulation is done for checking the anti-interference capability of system when there is noise existing in output.

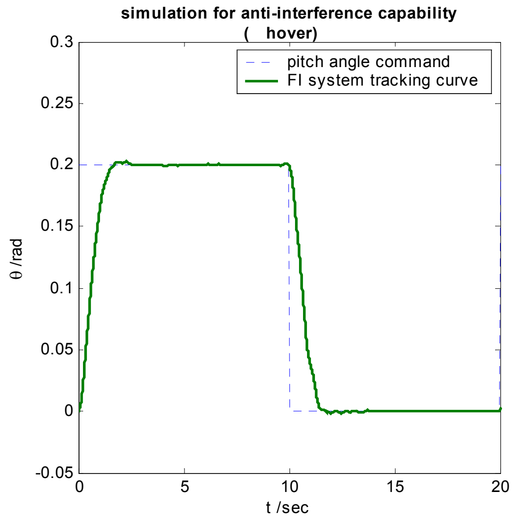

Fig. 8-a. Simulation for fault-tolerance ability in FI system

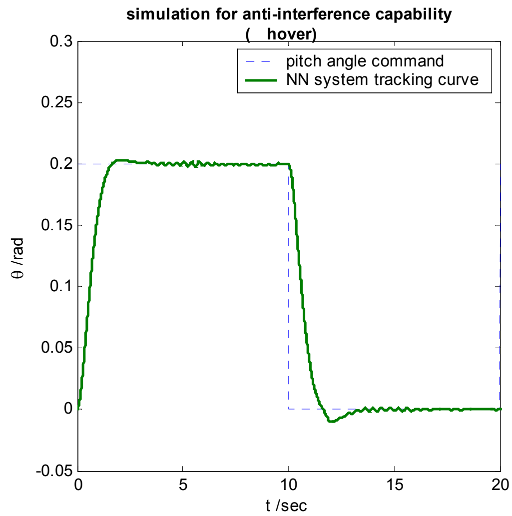

Fig. 8-b. Simulation for fault-tolerance ability in NN system

Fig. 8-a and Fig. 8-b show the response curves of FI system and NN system at hover, while the gauss white noise exists in pitch angle output. The response curves of both FI system and NN system are affected by the output noise (The effect to original system is stronger than FI system and NN system, considering the definition of figure, the original system response curves are not shown). As shown in figures, the

effect of FI system response curve (Fig. 8-a) is better than that of NN system (Fig. 8-b) and could still track command well to achieve the demands of ACAH.

5.4 Simulation for three-axis uncoupled control

The simulation is done for checking the three-axis uncoupled performance of FI system for ACAH response type. The structure of FI system for three-axis attitude channels could be gained as shown in Fig. 9, in which the Fuzzy Immune Control Block $\_\theta/\phi/\psi$ is established based on the single channel system structure shown in Fig. 1. θ is the pitch angle, ϕ is the roll angle, and ψ is the yaw angle. Once achieving design, all control parameters of the systems keep invariable.

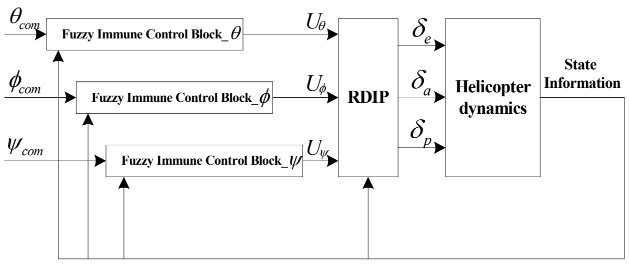

Fig. 9.Structure of FI system for three-axis uncoupled control

Fig. 10~11 show the three-axis attitude response curves of FI system at 20knots and 60knots forward flight respectively. In Fig. 10, the command of pitch angle θ_{com} is a step signal with the value 0.1rad, ϕ_{com} is a step signal with the value 0.2rad, and ψ_{com} is zero. In Fig. 11, θ_{com} is 0.2rad, ϕ_{com} is 0.1rad, and ψ_{com} is zero. It is clear from the figures that FI system can implement the three-axis uncoupled control well and track the three-axis attitude commands accurately.

Among the experiments in section 5.1~5.3, the simulation time is 20 seconds and the sample time is 0.01 second. Results show the actual running time of FI system is 8~10 seconds, and NN system is 19~22 seconds respectively. It indicates that the real-time performance of FI system is much better than NN system.

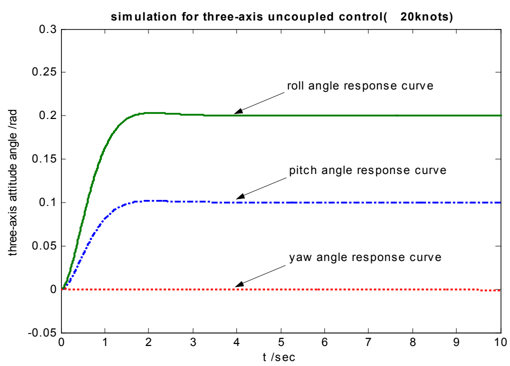

Fig. 10. Simulation for three-axis uncouple control (20knots)

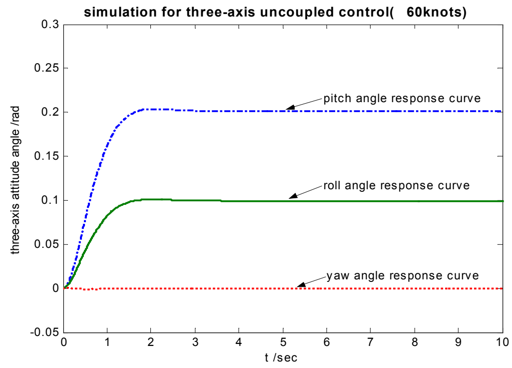

Fig. 11. Simulation for three-axis uncouple control (60knots)

6. CONCLUSIONS

FIAMIC scheme is proposed helicopter for LFEC problem in this paper. Results comparing with NNAMIC method show the feasibility and advantages of the proposed scheme. It is a profitable new trying on combination of AIS theory and traditional control methods. This method could also be generalized to flight control problem of other vehicles.

The work is supported under National Science Fund of China with the grant number 60774061.

REFERENCES

Nakwan K. and Anthony J.C. (2004). Adaptive Output Feedback for Altitude Control of an Unmanned Helicopter Using Rotor RPM. *AIAA paper,* 2004-5323.

Nilesh A.S. and Joseph F.H. (2004). Adaptive model inversion control of a helicopter with structural load limiting. *AIAA paper,* 2004-4753.

Takahashi K. and Yamada T. (1998). Application of an immune feedback mechanism to control systems. *JSME International Journal,* Series C, **41(2)**, 184-191.

Jun Li, Hui Yan and Guoqing Tang (2004). Simulation Study of the Series Active Power Filter Based on Nonlinear Immune Control Theory. *Proceedings of the 2004 IEEE International Conference on Electric Utility Deregulation, Restructuring and Power Technologies Hong Kong: DRPT,* 758-762.

Liu Liqun and Sun Zhiyi (2007). Application of immune response feedback principle to hydraulic turbine system. *Journal of System Simulation,* **19(7)**, 1579-1582.

Anon (2000). *Aeronautical design standard ADS-33E handling qualities requirements for military helicopters*. US Army, St. Louis, MO, USA.